Arch. Mech., 44, 5–6, pp. 563–584, Warszawa 1992

Modelling of large plastic deformations based on the mechanism of micro-shear banding. Physical foundations and theoretical description in plane strain

R. B. PĘCHERSKI (WARSZAWA)

SHEAR BANDING is related with large plastic deformations produced by mechanisms of crystallographic slip and/or twinning and micro-shear. Physical foundations and motivations to formulate simplified phenomenological model are considered. Plane deformations of elastoplastic material accounting for micro-shear bands are studied. The derived relations show that micro-shear bands produce the non-coaxiality between principal directions of stress and rate of plastic deformations. It transpires that, depending on the contribution of the mechanisms involved in plastic flow, a fully active range, separated from the elastic range by a truly nonlinear zone called the partially active range, may exist. In case of continued plastic flow with the deviations from proportional loading contained within the fully active range the incremental plastic response is linear, whereas the constitutive relations derived for the partially active range appear thoroughly nonlinear. Relations to known nonlinear flow laws in rates of deformation and stress are discussed.

1. Introduction

LARGE PLASTIC deformations of polycrystalline metallic materials, in particular under highly constrained conditions such as rolling or in the case of ductile fracture, while coalescence of voids occurs, can give rise to profuse flow localization into shear bands. They appear on different scales: grain-scale shear bands, sometimes called *micro-shear bands*, which extend through a few grains; and sample-scale shear bands, often called *macroscopic shear bands*, which extend through the entire sample. The so-called "shear banding" is related with plastic deformations produced by the competing mechanisms of crystallographic slip and/or twinning and micro-shear. The study will be confined to plane deformations of polycrystalline metallic materials at moderate temperature and quasi-static loading conditions. According to DÈVE and ASARO [1], in heavily deformed metals, shear localization progressively replaces the current deformation mode, *viz.* slip and/or twinning. This change in deformation mode contributes to the development of strain-induced anisotropy and modifies material properties. Therefore, formulation of a model of large plastic deformations accounting for micro-shear bands seems to be important for adequate constitutive description of inelastic behaviour of metallic materials. The model of plastic flow for a single-shearing system was considered in [2], whereas the model including double-shearing under loading conditions that do not deviate much from the proportional loading path was presented in [3]. In [4] the thoroughly nonlinear flow laws were presented that take into account micro-shear bands by means of double-shearing system.

The aim of the paper is to study the basic physical mechanisms of micro-shear banding and discuss physical motivation to formulate a phenomenological model of plastic flow accounting for micro-shear bands. The effect of micro-shear bands is modelled by means of double-shearing system. The model proposed shows that micro-shear bands

produce the non-coaxiality between principal directions of stress and rate of plastic deformations. It turns out that, depending on the contribution of the mechanisms involved in plastic flow, a *fully active range*, separated from the elastic range by a truly nonlinear zone called the *partially active range*, may exist. A new physical insight is given into the linear and nonlinear flow laws, in rates of deformations and stress, known in the theory of plasticity. The idea of multiple potential surfaces forming a vertex on the smooth yield surface studied earlier by MRÓZ [5] is applied here to connect the *fully active range* and the *partially active range* with the definite geometric pattern of micro-shear bands. In case of continued plastic flow with the deviations from proportional loading contained within the *fully active range* the incremental plastic response is linear and the term responsible for the non-coaxiality produced by the micro-shear bands is formally similar to the Mandel–Spencer non-coaxiality effect discussed e.g. by NEMAT-NASSER *et al.* [6], NEMAT-NASSER [7] and LORET [8] within the context of plastic behaviour of single crystals or geological materials. The constitutive relations derived for the *partially active range* correspond to a special case of the nonlinear flow laws studied earlier, within the framework of infinitesimal strains, by KLYUSHNIKOW [9], HILL [10], ILYUSHIN [11] and MRÓZ [12].

2. Basic physical mechanisms

Plastic deformation of metal crystals has long been known to occur by the development of discrete shear slip steps visible on the surface of the polished specimen with a light microscope or even by the naked eye as one or more sets of parallel fine lines called slip lines. The application of higher magnification by means of the electron microscope shows that what appears as a line, or at best a narrow slip band in the light microscope, can be resolved by the electron microscope as discrete slip lamellae. These lamellae result from microscopic shear movements along well-defined crystallographic planes, that are referred to as slip or glide planes. According to the nomenclature in NEUHÄUSER [13], the slip line corresponds to each slip step in the slip band which is supposed to be produced by the movement of closely correlated dislocations in a moving dislocation group. Several slip lines are thus clustered to form a slip band. Often the slip bands are again clustered in units called slip band bundles. The activation of new slip bands appears at a considerable distance from the neighbouring bundle. The activation of new slip bands at a long distance from preexisting ones and the growth of slip band bundles up to a certain slip-band density often results in the propagation of a so-called Lüders band. Certain hierarchy of plastic slip from slip lines to slip bands, to slip band bundles and to the propagating modes of shear accompanied by instabilities in time indicating the importance of collective, cooperative effects in dislocation generation and motion, is observed. These modes of shear are observed as coarse slip bands, Lüders bands, Portevin–LeChatelier bands and shear bands (cf. NEUHÄUSER [13], [14]).

The early observations of microscopic and macroscopic shear band formation in different metals and alloys are reported by GIL SEVILLANO *et al.* [15]. The papers of EMBURY *et al.* [16] and HATHERLY and MALIN [17], as well as, KORBEL *et al.* [18] and HARREN *et al.* [19] provide vast number of experimental results, obtained with the application of different techniques for different materials, which can shed more light on the mechanisms and hierarchy of shear band localization processes. Usually, the following terminology is used (cf. [1], [13-15] and KORBEL and MARTIN [20]):

Microband; *a long thin band, parallel to crystallographic slip planes, often formed across the width of the grain. (The distinct markings on the surface produced by the microbands are called sometimes* ***coarse slip bands****).*

Micro-shear band; *a long and thin sheet-like region of concentrated plastic shear crossing grain boundaries without deviation and forming a definite pattern in relation to the principal directions of strain. It bears very large shear strains and lies in a position that is usually non-crystallographic. This means that micro-shear bands are not parallel with a particular slip plane of the crystallites they intersect.*

The studies of the mechanisms of plastic deformations carried out by KORBEL [21], and SZCZERBA and KORBEL [22] as well as by KORBEL and MARTIN [20] and BOCHNIAK [23] can lead to the conclusion that in crystalline materials subjected to large strain, and in particular in situations of change in deformation path, the Lüders bands, Portevin–LeChatelier bands and shear bands, originate in the same mechanism. This mechanism is related to the time and spatial organization of dislocations, avalanche-like movement of dislocation groups and formation of micro-shear bands which take non-crystallographic orientations and may cross grain boundaries without change of their direction, often with an extremely high speed. According to KORBEL [21], dynamic properties of the dislocation groups enable the propagation of the plastic deformation initiated in the coarse slip band into the neighbouring grains in the form of micro-shear bands. If the groups of co-planar dislocations, emitted from the dislocation sources and gliding on the slip planes organized in a slip band, are suddenly stopped by the grain boundaries, the kinetic energy of the groups may become either scattered or converted into elastic-plastic impulses, called in [21] *plastons*, which conserve a substantial fraction of the energy spread into the neighbouring grain and continue to realize the plastic deformation without changing the direction of their course (micro-shear bands). The formation of *plaston* in terms of the high-amplitude shear stress wave impulse interacting with a strong obstacle (grain boundary) was studied by PAWEŁEK and KORBEL [24] within the framework of the soliton-like behaviour of a moving dislocation groups.

As it was stressed in DUGGAN *et al.* [25] and HATHERLY and MALIN [17], a particular micro-shear band operates only once and develops rapidly to its full width. The micro-shear bands, once formed, do not contribute further to the deformation process. Thus, it appears that the successive generations of active micro-shear bands competing with the mechanisms of crystallographic slip and/or twinning are responsible for the process of plastic flow. Also observations of DUBOIS [26] and DUBOIS *et al.* [27], concerning the initiation and evolution of micro-shear bands in polycrystalline sheet of pure copper subjected to rolling, confirm the sequential character of the active micro-shear bands as carriers of large plastic strain. Application of the fiducial grid technique and scanning electron microscopy made it possible to observe simultaneously traces of slip lines and coarse slip bands, as well as the grid and some grain boundaries sheared off by active micro-shear bands initiated at different stages of deformation process. The mean angle between the observed micro-shear bands and the rolling axis was nearly $\pm 35°$. The same methodology was used also by YANG [28] and REY [29] to study the substructure and the sequential character of active shear bands in a single crystal and bicrystals. The authors in [15] argue that at least during part of the deformation the strain can be entirely or almost entirely concentrated in the shear bands. On the other hand, YEUNG and DUGGAN [30] studied the question of the contribution that active micro-shear bands make to accommodate the total imposed strain on the example of rolling of 70/30 brass

slab. Applying the geometrical model of shear banding developed in [15] and introducing the fraction of the plastic deformation increment carried by active micro-shear bands they have found experimentally that this fraction changes very irregularly in deformation and in different locations along the specimen. The mean value of the fraction parameter lies between 0.6 and 0.8. According to [17] the shear bands formed in rolling are usually inclined by about $\pm 35°$ to the rolling plane and are orthogonal to the specimen lateral face, although there can be considerable deviations from this value within the 15° to 50° range. The problem of specifying the angle is complicated by the difficulty of distinguishing the most recently formed shear bands from those that were formed earlier and subsequently rotated with material towards the rolling plane.

According to the discussion in [15] and [17], as well as in [19] and [26], the amount of strain prior to the appearance of the micro-shear bands (threshold strain) and also the aspect, size and volume fraction of the micro-shear bands depend strongly on the stacking fault energy (SFE) of the material.

(i) In high stacking fault energy FCC metals (SFE > 40 mJ/m^2) the threshold strain ϵ_{th} is high, whereas the volume fraction of the micro-shear bands is low. In copper, with SFE ≈ 60 mJ/ m^2, the equivalent figures by rolling are $\epsilon_{th} \approx 1$ and the volume fraction is about 5% for $\epsilon \approx 3$. A similar behaviour is observed in BCC metals. For example, in iron the first micro-shear bands are observed at $\epsilon_{th} \approx 1.3$ and the rate of increase of micro-shear bands within the volume is very much less so that at $\epsilon \approx 2$ the volume fraction is about 3%. On the other hand, the investigations of aluminum killed steel, containing 0.06 wt% C subjected to predeformation by means of rolling and subsequent tension in parallel and perpendicular tension axis to the rolling direction reveal that the first micro-shear bands appear at very low tensile strain, about 0.01, [20].This shows that the change of deformation path can diminish greatly the threshold strain of micro-shear banding. Further studies are necessary to shed more light on this important problem.

(ii) In materials with low stacking fault energy threshold strain is low and the volume occupied by micro-shear bands increases rapidly with strain, e.g. in 70/30 brass with 15 mJ/m^2, subjected to rolling micro-shear bands form first at $\epsilon_{th} \approx 0.80$ (50% rolling reduction). Thereafter, plastic deformation takes the form of micro-shear bands formation up to very large strain ($\epsilon \approx 3$). Each band undergoes high shear strains, up to $\gamma \approx 10$. New micro-shear bands appear as deformation continues. Consequently, the sheared volume steadily increases and continues to form until at $\epsilon \approx 3$ almost 90% of the total volume has been traversed by micro-shear bands. In copper — 8.8 at% silicon, with SFE ≈ 3 mJ/m^2, first micro-shear bands appear at $\epsilon_{th} \approx 0.40$.

As it is reported in [17], in some cases, two sets of bands intersecting each other were observed, whereas in other cases only one set is present, or in some parts of the structure there is one set and in other part there are two sets. In the case of FCC metals of low stacking fault energy, two sets of shear bands form an array of rhomboidal prisms with axes parallel to the transverse direction. Shear bands of each sign exist together in any particular material volume. In the FCC metals of medium or high stacking fault energy as well as in BCC metals only one set of shear bands forms in a particular volume and neighbouring volumes develop bands of opposite sign. The volume concerned usually consists of several grains. Similar shear band systems were observed also in plane-strain tension and compression tests. ANAND and SPITZIG [31] conducted experiments on a maraging steel and examined with use of light microscopy the polished and etched cross-sections taken from the middle of the tension and compression specimens deformed to various

values of strain. Narrow shear bands were first detected in both tension and compression specimens when they were deformed to the strain just beyond that corresponding to diffuse necking in plane-strain tension test. The threshold logarithmic strain is, in this case, equal to about 0.034. These bands were approximately 1 to 2 μm wide. The inclination of the bands are reported to form at angles $\pm(38 \pm 2)^\circ$ about the maximum principal stress, the maximum principal stress being zero for the compression test. This angle did not appear to change with increasing strain.

Physical nature of shear banding is not yet completely explained. In particular, mechanisms of initiation and propagation of micro-shear bands across grain boundaries is a little known process. The discussed time and spatial organization of dislocations and the hierarchy of plastic slip processes from coplanar dislocation groups moving along active slip systems throughout slip lamellae and slip bands to coarse slip bands and micro-shear bands shows that crystalline solid subjected to plastic deformations can be considered as a complex hierarchically organized system. The description can be done at various levels which are, however, interconnected with each other. The microscopic, mezoscopic and macroscopic levels of approach can be distinguished. Each level of the description is related with pertinent state variables and a representative volume element (r.v.e.). It is still an open and challenging question how to apply this general guidelines to the particular physical situation of shear banding. Nevertheless, the reported observations can make the basis to formulate a tentative, phenomenological model of large plastic deformations accounting for micro-shear bands.

3. Physical motivation to formulate simplified phenomenological model

The physical constraint on any continuum mechanics approach to metal plasticity, i.e. the physical dimension of the smallest r.v.e. of crystalline material for which it is possible to define significant overall measures of stress and strain during plastic deformation was thoroughly discussed by HILL [32], and HAVNER [33, 34]. According to [32], p. 8: "... the dimensions must be large compared with the thickness of the glide packets separating the active glide lamellae (generally of order 10^{-4} cm in many metals at ordinary temperatures). Thus, the linear dimension of the smallest crystal whose behaviour can legitimately be considered from the standpoint of the theory of plasticity is probably of order 10^{-3} cm." On the other hand, HAVNER [33] argues that, to an observer who can resolve distances to 1 μm, the deformation of crystal grains (with the mean grain diameter of order 100 μm) within plastically deformed metal polycrystals is relatively smooth. At such scale of observation, called *microscopic level*, one can just distinguish between slip lines on crystal surfaces. These slip lines appear on the *submicroscopic level* as slip line bundles and slip bands of order 0.1 μm width, containing numerous glide lamellae between which amounts of slip as great as 10^3 lattice spacings have occurred. On the *submicroscopic level* the observer, resolving distance to 10 nm (the order of 100 atomic spacings), is aware of highly inhomogeneous and discontinuous deformation within each grain. "Hence a continuum point-of-view at this second level would seem untenable" (cf. [33], p. 93). Therefore, the minimum physical dimension of the r.v.e. in the continuum microscopis description of elastic-plastic deformations of crystalline solids is taken in [33] to be of the order 1 μm, i.e. $> 10^3$ lattice spacings. The linear dimension of the r.v.e. corresponding to the *macroscopic level* is often assumed of the order of 1 mm, for moderately fine-grained metals, [34]. This discussion is

values of strain. Narrow shear bands were first detected in both tension and compression specimens when they were deformed to the strain just beyond that corresponding to diffuse necking in plane-strain tension test. The threshold logarithmic strain is, in this case, equal to about 0.034. These bands were approximately 1 to 2 μm wide. The inclination of the bands are reported to form at angles $\pm(38 \pm 2)^\circ$ about the maximum principal stress, the maximum principal stress being zero for the compression test. This angle did not appear to change with increasing strain.

Physical nature of shear banding is not yet completely explained. In particular, mechanisms of initiation and propagation of micro-shear bands across grain boundaries is a little known process. The discussed time and spatial organization of dislocations and the hierarchy of plastic slip processes from coplanar dislocation groups moving along active slip systems throughout slip lamellae and slip bands to coarse slip bands and micro-shear bands shows that crystalline solid subjected to plastic deformations can be considered as a complex hierarchically organized system. The description can be done at various levels which are, however, interconnected with each other. The microscopic, mezoscopic and macroscopic levels of approach can be distinguished. Each level of the description is related with pertinent state variables and a representative volume element (r.v.e.). It is still an open and challenging question how to apply this general guidelines to the particular physical situation of shear banding. Nevertheless, the reported observations can make the basis to formulate a tentative, phenomenological model of large plastic deformations accounting for micro-shear bands.

3. Physical motivation to formulate simplified phenomenological model

The physical constraint on any continuum mechanics approach to metal plasticity, i.e. the physical dimension of the smallest r.v.e. of crystalline material for which it is possible to define significant overall measures of stress and strain during plastic deformation was thoroughly discussed by HILL [32], and HAVNER [33, 34]. According to [32], p. 8: "... the dimensions must be large compared with the thickness of the glide packets separating the active glide lamellae (generally of order 10^{-4} cm in many metals at ordinary temperatures). Thus, the linear dimension of the smallest crystal whose behaviour can legitimately be considered from the standpoint of the theory of plasticity is probably of order 10^{-3} cm." On the other hand, HAVNER [33] argues that, to an observer who can resolve distances to 1 μm, the deformation of crystal grains (with the mean grain diameter of order 100 μm) within plastically deformed metal polycrystals is relatively smooth. At such scale of observation, called *microscopic level*, one can just distinguish between slip lines on crystal surfaces. These slip lines appear on the *submicroscopic level* as slip line bundles and slip bands of order 0.1 μm width, containing numerous glide lamellae between which amounts of slip as great as 10^3 lattice spacings have occurred. On the *submicroscopic level* the observer, resolving distance to 10 nm (the order of 100 atomic spacings), is aware of highly inhomogeneous and discontinuous deformation within each grain. "Hence a continuum point-of-view at this second level would seem untenable" (cf. [33], p. 93). Therefore, the minimum physical dimension of the r.v.e. in the continuum microscopis description of elastic-plastic deformations of crystalline solids is taken in [33] to be of the order 1 μm, i.e. $> 10^3$ lattice spacings. The linear dimension of the r.v.e. corresponding to the *macroscopic level* is often assumed of the order of 1 mm, for moderately fine-grained metals, [34]. This discussion is

4. Fundamentals and basic equations

4.1. Fundamentals

ASSUMPTION 1

Motivated in the single crystal plasticity, it is assumed that the distinction should be made between the kinematics of the continuum and the kinematics of the underlying substructure.

In plasticity of single crystals, it is evident that the dislocations traversing a volume element produce a change of its shape but they do not change its lattice orientation. The macroscopic counterpart of such a situation in finite deformation plasticity of polycrystals is the Mandel's concept of the intermediate relaxed configuration, called isoclinic, in which the chosen director frame always keeps the same orientation with respect to the fixed axis (cf. e.g. TEODOSIU [41], MANDEL [37], and KRATOCHVIL [42], as well as, KLEIBER and RANIECKI [43] and the recent papers by RANIECKI and SAMANTA [44] and RANIECKI and MRÓZ [45]). CLEJA–TIGOIU and SOÓS[46] presented a critical review of the papers which led to the formulation of the fundamental ideas of the elastoviscoplastic and, in particular, elastoplastic models for metals based on the following assumption:

ASSUMPTION 2

There exist the local, relaxed, isoclinic configurations, resulting in the unique decomposition of gradient $\mathbf{F}$ into the elastic component $\mathbf{E}$ and the plastic one $\mathbf{P}$:

$$\mathbf{F} = \mathbf{EP}. \tag{4.1}$$

It is typical for most of the deformed metallic solids that their distortional elastic strains remain small under arbitrary loading conditions, whereas they can undergo large elastic dilatational changes in shape under very high pressure. RANIECKI and NGUYEN [47] have shown, studying thermomechanics of isotropic elasto-plastic solids at finite strain and arbitrary pressure, that the tensor of elastic moduli in Eulerian description can be expressed in terms of derivations of the free energy as simply as in the case of infinitesimal strains, provided the logarithmic elastic strain $\boldsymbol{\varepsilon} = \ln \mathbf{V}^e$ is adopted as a state variable and that the values of the ratios of principal elastic stretches $\mathbf{U}^e$, from the polar decomposition $\mathbf{E} = \mathbf{V}^e\mathbf{R}^s = \mathbf{R}^s\mathbf{U}^e$, are limited in the interval [5/6, 7/6]. The thermomechanic theory of isotropic elastic-plastic solids for small distortional elastic strains but arbitrary elastic dilatational changes, developed in [47], is based on the assumption:

ASSUMPTION 3

(i) metallic solids are plastically incompressible;

(ii) an elastic response is not influenced by prior plastic straining;

(iii) elastic distortional response of metallic solid is linear.

Similarly as in [48] and [49], the conjecture is made here that the Assumption 3 holds also, at least as a first approximation, in the case of elastic-plastic solid with deformation-induced anisotropy produced by micro-shear bands.

Before discussing the appropriate plastic flow law it is important to be precise about the meaning of "yield" in the present context. The precise connection of the nominal yield points with intrinsic material properties was discussed by HILL [35, 50]. Consider a representative volume element of the polycrystalline aggregate being initially at zero load and afterwards subjected to macroscopically uniform deformations by means of radial

loading paths with the Cauchy stress varying monotonically the Cartesian components in fixed ratios. A limit domain boundary in stress space can be determined. Along each ray in the stress space, the representative volume element is loaded beyond the material's elastic response to a small predetermined residual strain. Repeating the procedure along the various rays and connecting the points thus obtained, we can approximate a surface which is the locus of the elastic regime associated with the given residual strain specifying the onset of plastic yielding. The first locus, related with a virgin state is termed the *initial yield surface* and the other ones are called the *subsequent yield surfaces*. These surfaces are shown to translate and distort as the history of plastic flow evolves. There is ample experimental evidence showing that the shape of *yield surfaces* grossly depends on the residual strain value (cf e.g. HECKER [51] and IKEGAMI [52]).

HILL [50] considered the elastic domain in stress space by exploratory "unloading" from the current stress state, i.e. by elastic paths to states where further plastic strains become observable in a few grains and called such a domain boundary the *elastic limit*, reserving the term *yield surface* to represent the locus of *yield points* obtained by further plastic deformation from a point on the current *elastic limit* produced by increasing monotonically proportional loading, till the state is reached when further glide hardening is suspended on every slip system in every grain. The macro-stress on this path would still increase, as progressively more of the polycrystalline aggregate becomes plastic, tending asymptotically to an upper bound that could be closely approached within a strain of order about 10^{-3}, due to elastic constraint. Technically the yield point is obtained by a backward extrapolation of the experimental data from the portion of the loading part beyond a very small strain of about 10^{-3}. Such *yield points* depend only on the critical stresses for glide on potential systems throughout the polycrystalline aggregate and, in particular, unlike the *elastic limit*, it is independent of the micro-stress distribution under the current loading. An alternative term *extremal surface* was coined in [35] to emphasize its characteristic property. The idea of *extremal surface* is related with the concept of *eigenmodes*, which has been introduced in [35] in the following way. Assume that after a given prestrain of the representative volume element of the polycrystalline aggregate, further glide hardening on the active slip systems of its constituent grains is suspended. In general, due to constraint hardening, the incremental plastic flow under constant overall load is still precluded. However, as it is observed in [35], special configurations of the internal stresses and yield vertices are possible that together admit one or more fields of strain rate η, which is compatible with zero stress rate. Such fields, if macroscopically uniform, were called *eigenmodes* and the pertinent stress field is the *stress eigenstate* (cf. HILL [53] where the eigenmodal deformations in elastic-plastic continua were studied).

OBSERVATION 3

If the micro-shear bands are understood as an effect of the special configuration of internal micro-stresses that accumulate at grain boundaries till the glide hardening on the active slip systems is suspended and then abruptly release producing, under constant overall load, the field of plastic strain rate $\mathbf{D}_{MS}$, the striking correspondence with the eigenmodes discussed in [35] can be observed.

As it is emphasized in [35], the *extremal surface* is not a single yield surface but is rather an assemblage of yield points for physically distinct states of the representative volume element, none of which can be reached from any other via purely elastic paths in the stress space. Accordingly, the stress space can be divided into the following three

regions:

(i) an elastic region enclosed by the *elastic limit*,

(ii) an intermediate plastic region where only very small strains appear and which lies outside the *elastic limit* but is enclosed by the *extremal surface*,

(iii) a plastic region which lies outside the *extremal surface* and where larger strains appear (larger compared to those appearing in the intermediate region).

OBSERVATION 4

The properties of the *extremal surface* conform very well with the mechanisms of micro-shear banding. The yield state approaching certain eigenstate on the *extremal surface* can be related with the formation of a particular spatial pattern of micro-shear bands. The other state occupying the *extremal surface* pertains to the other spatial pattern of micro-shear bands. The transition from the one state to the other one is not possible via purely elastic path, for an accumulated plastic strain is necessary to produce the new set of micro-shear bands characterized, in general, by the other geometric pattern.

The aforementioned discussion shows that the complete description of elastic-plastic behaviour of metallic solids requires a model with two characteristic surfaces, which can be introduced at each step of the plastic deformation process; the *extremal surface* taking into account, in general, textural anisotropy and the internal *yield surface* related with back stress anisotropy (cf. eg. MRÓZ and NIEMUNIS [54]). As the first step, however, the model based on the following assumption will be developed here:

ASSUMPTION 4

The one-surface model, related with the *extremal surface* and dealing with processes of advanced plastic deformations produced from the outset by two competing mechanisms

(i) crystallographic multiple slip,

(ii) micro-shear banding is assumed.

Such a model can be useful for the analysis of the deformation processes, in which advanced plastic strains play essential role.

4.2. Basic equations

ASSUMPTION 5

The simple model of small distortional and dilatational elastic strains and finite plastic deformations with Huber–Mises yield criterion approximating the *extremal surface*

$$f = \bar{\tau} - \kappa(\bar{\gamma}) = 0 \tag{4.2}$$

is applied at hand to incorporate new effects of active micro-shear bands, where

$$J_2 = \frac{1}{2}\boldsymbol{\tau}' : \boldsymbol{\tau}', \quad \bar{\tau} = (J_2)^{1/2}, \quad \bar{\gamma} = \int_0^t \dot{\bar{\gamma}}\, dt, \quad \dot{\bar{\gamma}} = (2\mathbf{D}^p : \mathbf{D}^p)^{1/2} \tag{4.3}$$

and $\boldsymbol{\tau}'$ is the deviator of the Kirchhoff stress, whereas $\bar{\gamma}$ and $\dot{\bar{\gamma}}$ represent effective shear strain and effective shear strain rate, respectively.

The polar decomposition $\mathbf{E} = \mathbf{V}^e\mathbf{R}^e$, with $\mathbf{V}^e = \mathbf{1} + \boldsymbol{\varepsilon}$, where $\|\boldsymbol{\varepsilon}\| \ll 1$, leads to

$$\mathbf{D} = \mathbf{D}^e + \mathbf{D}^p, \quad \mathbf{W} = \boldsymbol{\Omega} + \mathbf{W}^p, \tag{4.4}$$

$$\mathbf{D}^e = \overset{\circ}{\boldsymbol{\varepsilon}} = \dot{\boldsymbol{\varepsilon}} + \boldsymbol{\varepsilon}\boldsymbol{\Omega} - \boldsymbol{\Omega}\boldsymbol{\varepsilon}, \quad \mathbf{D}^p = \mathbf{R}^s\{\dot{\mathbf{P}}\mathbf{P}^{-1}\}_s(\mathbf{R}^s)^{-1}, \tag{4.5}$$

$$\Omega = \dot{\mathbf{R}}^s(\mathbf{R}^s)^{-1}, \quad \mathbf{W}^p = \mathbf{R}^s\{\dot{\mathbf{P}}\mathbf{P}^{-1}\}_a(\mathbf{R}^s)^{-1}, \tag{4.6}$$

where $\mathbf{R}^s$ is the rotation of substructure arising from elastic deformations and the geometric constraints imposed by boundary and compatibility conditions.

ASSUMPTION 6

The J_2 flow theory is assumed for the case when the sole mechanism of crystallographic multiple slip is responsible for plastic deformation.

REMARK 2

The discussion of the status of the classical laws *vis-à-vis* the latent eigenstates and the *extremal surface* is given in [35].

The pertinent flow law reads

$$\mathbf{D}^p_S = \langle\lambda\rangle\mathbf{N} = \frac{\sqrt{2}}{2}\dot{\bar{\gamma}}_S\mathbf{N}, \tag{4.7}$$

where

$$\dot{\bar{\gamma}}_S = \sqrt{2}\langle\lambda\rangle, \quad \mathbf{N} = \frac{\boldsymbol{\tau}'}{\sqrt{2}\bar{\tau}}. \tag{4.8}$$

Due to (4.4) the total rate of deformation reads

$$\mathbf{D} = \mathbf{D}^e + \mathbf{D}^p_S = (\mathcal{L}^{-1} + \frac{\alpha}{2h}\mathbf{N}\otimes\mathbf{N}) : \overset{\circ}{\boldsymbol{\tau}}, \quad \text{for} \quad \mathbf{D}^p = \mathbf{D}^p_S, \tag{4.9}$$

where $h = \partial\kappa/\partial\bar{\gamma}$ denotes plastic hardening modulus, $\lambda = \dfrac{\overset{\circ}{\boldsymbol{\tau}}\cdot\mathbf{N}}{2h}$ is the loading index, whereas $\dot{\bar{\gamma}}_S$ corresponds to the effective shear strain rate produced by the sole mechanism of multiple slip, and $\mathcal{L}$ represents the tensor of elastic moduli. The bracket $\langle\cdot\rangle$ and α give, respectively, $\langle\lambda\rangle = \lambda$; $\alpha = 1$ if $\lambda > 0$ and $f = 0$ and $\langle\lambda\rangle = 0$; $\alpha = 0$ if $\lambda \leq 0$ or $f < 0$. The substructure corotational objective rate of the Kirchhoff stress τ is given by

$$\overset{\circ}{\boldsymbol{\tau}} = \dot{\boldsymbol{\tau}} - \Omega\boldsymbol{\tau} + \boldsymbol{\tau}\Omega, \quad \Omega = \mathbf{W} - \mathbf{W}^p, \tag{4.10}$$

provided $\mathbf{W}^p \neq \mathbf{0}$. In case of the J_2 flow theory, with isotropic hardening, $\mathbf{W}^p = \mathbf{0}$.

5. Phenomenological model of plastic flow accounting for a double shear system

To capture the gross effects of active micro-shear bands, consider the mode of plane deformation of rigid-plastic solid. The contribution of the mechanisms of crystalographic multiple slip is approximated, in the simplest case, by the flow rule (4.7). The rate of plastic deformations consists, in such a case, of a pure shear in the plane of plastic flow and, for isotropic material, the state of stress at each point is a pure shear stress

$$\tau = \frac{1}{2}(\tau_1 - \tau_2), \tag{5.1}$$

together with the hydrostatic component of the stress tensor whose value is equal to

$$\tau_3 = \frac{1}{2}(\tau_1 + \tau_2), \tag{5.2}$$

where τ_1, τ_2 are the principal stresses in the plane (x, y) of plastic flow and $\tau_3 = \tau_z$ is the stress normal to the plane (x, y). The principal stress components are ordered here

so that $\tau_1 \geq \tau_3 \geq \tau_2$. In such a case the principal axes of stress and rate of plastic deformations coincide, (cf. HILL [55], pp:129-130).

ASSUMPTION 7

The contribution of active micro-shear bands, with their definite geometric pattern, to rate of plastic deformations is idealized by means of an additional double-shearing system, normal to the flow plane, with the directions of shear $\mathbf{n}_1^{(i)}$ and the normal to the shear plane $\mathbf{n}_2^{(i)}$, $i = 1, 2$.

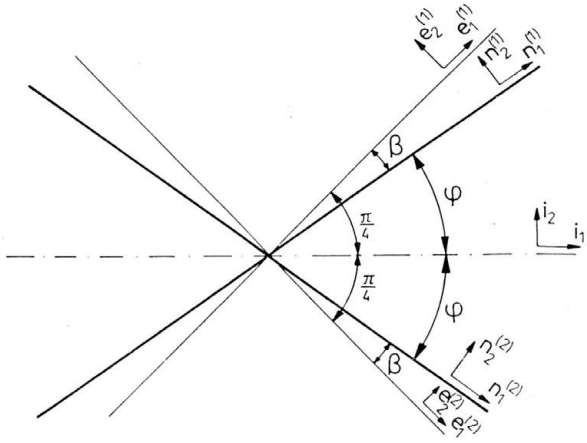

FIG. 1. Geometry of double shear system, $\beta = \frac{\pi}{4} - \varphi$; $\varphi \in \left(0, \frac{\pi}{2}\right)$.

The double-shearing system can be oriented according to the fixed principal axes of strain, (e.g. $\mathbf{i}_1$ may correspond to the direction of rolling, extrusion, tension or compression), cf. Fig. 1. In such a case the angle φ approximates the mean orientation of micro-shear bands. For a single crystal φ can be regarded as a crystalline parameter. For a polycrystalline aggregate the following assumption is made, cf. [6]:

ASSUMPTION 8

The angle φ is viewed as a statistically averaged, microscopically preferred, micro-shear bands orientation parameter characterizing and transmitting to the macroscopic level the geometry of their spatial pattern.

According to HILL [35], the macroscopic constitutive equations describing elastic-plastic deformations of polycrystalline aggregate are either thoroughly or partially incrementally nonlinear. Depending on the contribution of the mechanisms involved in plastic flow, a region of fully active loading called also a *fully active range*, separated from the total unloading (elastic) range by a truly nonlinear zone, corresponding to the *partially active range*, may exist. According to the works of HILL [35], PETRYK [39] and CHRISTOFFERSEN and HUTCHINSON [56] the following hypothesis is formulated:

HYPOTHESIS 1

For continued plastic flow with the deviations from proportional loading contained within certain cone of stress rates, that corresponds to the *fully active range*, the incremental plastic response can be assumed as linearly dependent on the stress increment. Outside

the range, the spatial pattern of active micro-shear bands is continuously changing when the partially active loading is varied. This is associated with the thoroughly nonlinear relation between the rates of plastic deformations and stress.

Accordingly, for the loading paths within the *fully active range* the principal directions of stress and strain are coaxial and it is then justified to relate the unit vectors of the double-shearing system $(\mathbf{n}_1^{(i)}, \mathbf{n}_2^{(i)})$ with the unit vectors $(\mathbf{e}_1^{(i)}, \mathbf{e}_2^{(i)})$, $i = 1, 2$, describing the orientation of the planes of maximum shear stress. According to the discussion in the Sec. 2., it is typical of active micro-shear bands that their planes are rotated relative to the respective planes of maximum shear stress by the angle $\beta \approx (5 \div 10)°$, (cf. Fig. 1).

REMARK 3

Such a misorientation is very characteristic for micro-shear bands produced in the deformation processes carried under nearly isothermal conditions. On the other hand, thermal shear bands, i.e. the mode of flow localization governed by a coupled thermo-plastic mechanism, the special case of which are so-called adiabatic shear bands, are often reported to coincide with slip lines and the trajectories of maximum shearing stress(cf. e.g. DODD and BAI[57]), what results in $\beta = 0$.

According to Fig. 1. the following geometrical relations hold

$$\begin{aligned} \mathbf{n}_1^{(1)} &= \cos\beta\mathbf{e}_1^{(1)} - \sin\beta\mathbf{e}_2^{(1)}, \quad \mathbf{n}_1^{(2)} = \cos\beta\mathbf{e}_1^{(2)} + \sin\beta\mathbf{e}_2^{(2)}, \\ \mathbf{n}_2^{(1)} &= \sin\beta\mathbf{e}_1^{(1)} + \cos\beta\mathbf{e}_2^{(1)}, \quad \mathbf{n}_2^{(2)} = -\sin\beta\mathbf{e}_1^{(2)} + \cos\beta\mathbf{e}_2^{(2)}, \end{aligned} \tag{5.3}$$

ASSUMPTION 9

The rate of plastic deformations and plastic spin produced by active micro-shear bands is assumed in the form, which is formally similar to the well known Taylor relations in plasticity of single crystals

$$\mathbf{D}_{MS}^p = \sum_{i=1}^{2} \dot{\gamma}_{MS}^{(i)} (\mathbf{n}_1^{(i)} \otimes \mathbf{n}_2^{(i)})_s, \quad \mathbf{W}_{MS}^p = \sum_{i=1}^{2} \dot{\gamma}_{MS}^{(i)} (\mathbf{n}_1^{(i)} \otimes \mathbf{n}_2^{(i)})_a, \tag{5.4}$$

where $\dot{\gamma}_{MS}^{i}$ is the rate of plastic shearing along the i-th direction of shear.

Equations (5.4) can be transformed with use of (5.3) into the following form (cf. ZBIB [58], where similar transformation but in a different physical context was applied)

$$\begin{aligned} \mathbf{D}_{MS}^p &= \cos 2\beta [\dot{\gamma}_{MS}^{(1)} (\mathbf{e}_1^{(1)} \otimes \mathbf{e}_2^{(1)})_s + \dot{\gamma}_{MS}^{(2)} (\mathbf{e}_1^{(2)} \otimes \mathbf{e}_2^{(2)})_s] \\ &\quad + \frac{1}{2} \sin 2\beta [\dot{\gamma}_{MS}^{(1)} (\mathbf{e}_1^{(1)} \otimes \mathbf{e}_1^{(1)} - \mathbf{e}_2^{(1)} \otimes \mathbf{e}_2^{(1)}) - \dot{\gamma}_{MS}^{(2)} (\mathbf{e}_1^{(2)} \otimes \mathbf{e}_1^{(2)} - \mathbf{e}_2^{(2)} \otimes \mathbf{e}_2^{(2)})], \end{aligned} \tag{5.5}$$

$$\mathbf{W}_{MS}^p = \dot{\gamma}_{MS}^{(1)} (\mathbf{e}_1^{(1)} \otimes \mathbf{e}_2^{(1)})_a + \dot{\gamma}_{MS}^{(2)} (\mathbf{e}_1^{(2)} \otimes \mathbf{e}_2^{(2)})_a. \tag{5.6}$$

Taking into account that $\mathbf{e}_1^{(1)} = \mathbf{e}_2^{(2)}$ and $\mathbf{e}_2^{(1)} = -\mathbf{e}_1^{(2)}$, (cf. Fig. 1), the relations (5.5) and (5.6) can be expressed in terms of the unit vectors $(\mathbf{e}_1^{(1)}, \mathbf{e}_2^{(1)})$

$$\mathbf{D}_{MS}^p = \frac{\sqrt{2}}{2} \dot{\gamma}_{MS} (\mathbf{e}_1^{(1)} \otimes \mathbf{e}_2^{(1)})_s + \dot{\epsilon}_{MS} \frac{1}{2} (\mathbf{e}_1^{(1)} \otimes \mathbf{e}_1^{(1)} - \mathbf{e}_2^{(1)} \otimes \mathbf{e}_2^{(1)}), \tag{5.7}$$

$$\mathbf{W}_{MS}^p = (\dot{\gamma}_{MS}^{(1)} + \dot{\gamma}_{MS}^{(2)}) (\mathbf{e}_1^{(1)} \otimes \mathbf{e}_2^{(1)})_a, \tag{5.8}$$

where

$$\dot{\gamma}_{MS} = \cos 2\beta (\dot{\gamma}_{MS}^{(1)} - \dot{\gamma}_{MS}^{(2)}), \quad \dot{\epsilon}_{MS} = \sin 2\beta (\dot{\gamma}_{MS}^{(1)} + \dot{\gamma}_{MS}^{(2)}), \tag{5.9}$$

represent, respectively, the rate of plastic shearing, $D_{12} = \dot{\gamma}_{MS}$, in the direction of the maximum shear stress, and the axial strain rate component in the direction $\mathbf{e}_1^{(1)}$, $D_{11} = -D_{22} = \dot{\epsilon}_{MS}$.

Let us observe that the contributions of the mechanisms of crystallographic multiple slip and micro-shear allow for the additive composition of the rates of plastic deformations as a combination of two modes of pure shear in the plane of plastic flow,

$$\mathbf{D}^p = \mathbf{D}^p_S + \mathbf{D}^p_{MS}. \tag{5.10}$$

Taking into account that in the case of plane deformations of incompressible plastic solid, the deviator of the Kirchhoff stress $\boldsymbol{\tau}'$ can be expressed by means of a pure shear stress, $\tau = \overline{\tau}$, and the generator produced by the unit vectors defining the plane of maximum shear stress $(\mathbf{e}_1^{(1)}, \mathbf{e}_2^{(1)})$,

$$\boldsymbol{\tau}' = 2\overline{\tau}(\mathbf{e}_1^{(1)} \otimes \mathbf{e}_2^{(1)})_s, \tag{5.11}$$

the relation for rate of plastic deformations reads

$$\mathbf{D}^p = \frac{\sqrt{2}}{2}\dot{\gamma}^*\mathbf{N} + \frac{\sqrt{2}}{2}\dot{\epsilon}_{MS}\mathbf{T}, \tag{5.12}$$

where

$$\dot{\gamma}^* = \dot{\overline{\gamma}}_s + \dot{\gamma}_{MS}, \tag{5.13}$$

and

$$\mathbf{N} = \sqrt{2}(\mathbf{e}_1^{(1)} \otimes \mathbf{e}_2^{(1)})_S, \quad \mathbf{T} = \frac{\sqrt{2}}{2}(\mathbf{e}_1^{(1)} \otimes \mathbf{e}_1^{(1)} - \mathbf{e}_2^{(1)} \otimes \mathbf{e}_2^{(1)}). \tag{5.14}$$

The unit tensor $\mathbf{T}$ is orthogonal to the normal $\mathbf{N}$ and coaxial with the tangent to the Huber–Mises yield locus in the deviatoric plane at the loading point (cf. Figs. 2 and 3)

$$\mathbf{T} = \Lambda\overline{\tau}\overset{\circ}{\left(\frac{\boldsymbol{\tau}'}{\overline{\tau}}\right)} = \Lambda[\overset{\circ}{\boldsymbol{\tau}}' - (\overset{\circ}{\boldsymbol{\tau}} : \mathbf{N})\mathbf{N}], \tag{5.15}$$

where, in the case of the pressure-insensitive Huber–Mises yield condition, the relation $\overset{\circ}{\boldsymbol{\tau}}' : \mathbf{N} = \overset{\circ}{\boldsymbol{\tau}} : \mathbf{N}$ is taken into account, and Λ is a normalization factor that is to be determined.

Observe that only the shearing component, $\dot{\gamma}^*$, of the rate of plastic deformations, $\mathbf{D}^p$, contributes to the change of the radius of the Huber–Mises yield locus. Then, the consistency condition, $\dot{f} = 0$, yields

$$\dot{\gamma}^* = \frac{\sqrt{2}}{2}\frac{\overset{\circ}{\boldsymbol{\tau}} : \mathbf{N}}{h}. \tag{5.16}$$

ASSUMPTION 10

The following *active micro-shear bands fractions* of the rate of plastic shearing, $f^{(1)}_{MS}$, $f^{(2)}_{MS}$, are introduced, respectively, to eliminate the unknown rates, $\dot{\gamma}^{(1)}_{MS}$, $\dot{\gamma}^{(2)}_{MS}$,

$$\dot{\gamma}^{(1)}_{MS}\cos 2\beta = f^{(1)}_{MS}\dot{\gamma}^*, \quad -\dot{\gamma}^{(2)}_{MS}\cos 2\beta = f^{(2)}_{MS}\dot{\gamma}^*, \tag{5.17}$$

where due to $(5.9)_1$, (5.13) and for $\dot{\gamma}^* > 0$ the following constraints hold

$$\frac{\dot{\overline{\gamma}}_S}{\dot{\gamma}^*} + f^{(1)}_{MS} + f^{(2)}_{MS} = 1, \quad f^{(1)}_{MS} + f^{(2)}_{MS} \in [0,1], \quad f^{(1)}_{MS}, f^{(2)}_{MS} \in [0,1]. \tag{5.18}$$

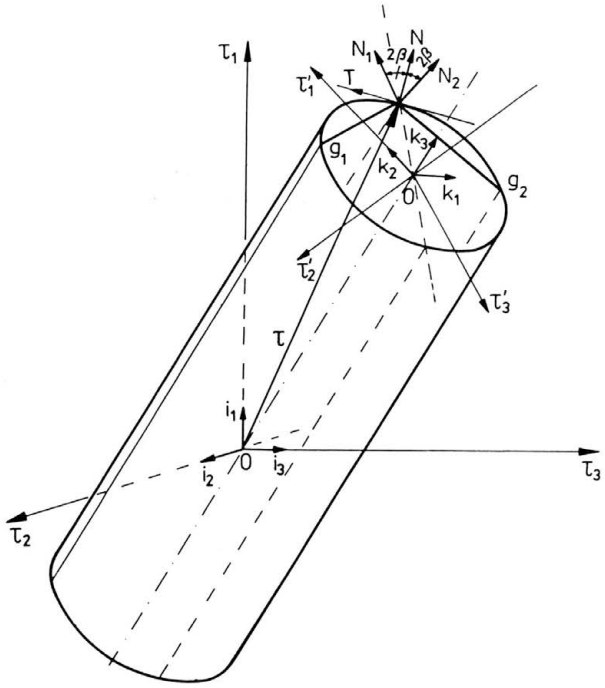

FIG. 2. Geometrical visualization of the yield surface and plastic potential planes in the three-dimensional space of principal stresses.

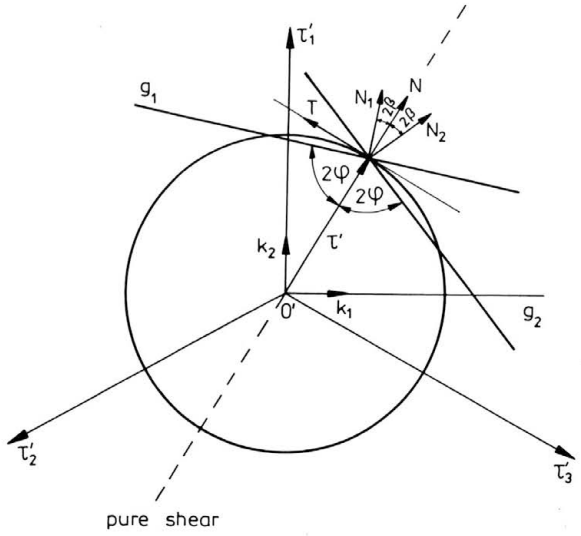

FIG. 3. Geometrical representation of the projections of the Huber-Mises cylinder and the potential planes, delimiting the *fully active range*, onto the π-plane (deviatoric plane).

Basing on the observation that the micro-shear bands can be active only in the case of continued plastic flow, i.e. when loading condition is fulfilled, it is assumed that for $\dot{\gamma}^* = 0$, $f^{(1)}_{MS} = f^{(2)}_{MS} = 0$.

The introduction of the fractions of the rate of plastic shearing, $f^{(1)}_{MS}$, $f^{(2)}_{MS}$, which are carried by the active micro-shear bands, opens a new possibility to account, on the *macroscopic level*, for the stochastic character of the micro-shear banding processes. This issue will be tackled in one of the subsequent points.

The following special cases result from the conditions (5.18)

(i) for $\dot{\bar{\gamma}}_S = 0$ and $\dot{\gamma}^* > 0$, $f^{(1)}_{MS} + f^{(2)}_{MS} = 1$ and, in particular, the limit cases can be reached

a) $f^{(1)}_{MS} = 0, \quad f^{(2)}_{MS} = 1, \quad \dot{\gamma}^* = -\dot{\gamma}^{(2)}_{MS} \cos 2\beta,$

b) $f^{(2)}_{MS} = 0, \quad f^{(1)}_{MS} = 1, \quad \dot{\gamma}^* = \dot{\gamma}^{(1)}_{MS} \cos 2\beta,$

(ii) for $\dot{\bar{\gamma}}_S = \dot{\gamma}^*$ and $\dot{\gamma}^* > 0$, $f^{(1)}_{MS} + f^{(2)}_{MS} = 0$ and due to $(5.18)_3$ $f^{(1)}_{MS} = f^{(2)}_{MS} = 0$, what results, according to (5.18), in $\dot{\gamma}^{(1)}_{MS} = \dot{\gamma}^{(2)}_{MS} = 0$.

According to (5.12) and (5.16) as well as from (5.15) and the Assumption 10, the following equation for the rate of plastic deformations is obtained,

$$\mathbf{D}^p = \frac{1}{2h}(\mathring{\boldsymbol{\tau}} : \mathbf{N})\mathbf{N} + \frac{\Lambda}{2h}(\mathring{\boldsymbol{\tau}} : \mathbf{N})(f^{(1)}_{MS} - f^{(2)}_{MS}) \tan 2\beta[\mathring{\boldsymbol{\tau}}' - (\mathring{\boldsymbol{\tau}} : \mathbf{N})\mathbf{N}]. \tag{5.19}$$

Due to the Assumption 4 the multiple sources of plasticity are dealt with and, accordingly, the theory of multimechanisms with multiple plastic potentials can be considered.

HYPOTHESIS 2

The following plastic potentials exist that are related with the respective mechanisms of plastic deformations:

(i) the plastic potential g_0 that reproduce at the *macroscopic level* the crystallographic multiple slips and is associated with the Huber–Mises yield function $g_0 = f$.

(ii) the non-associated plastic potentials g_1 and g_2 that approximate at the *macroscopic level* the multiplicity of plastic potential functions related with the separate active micro-shear bands.

The plastic potential functions g_1 and g_2 display the geometry of the assumed double-shearing system and result in two separate planes that form in the space of principal stresses τ_i, $i = 1, 2, 3$, a vertex at the loading point on the smooth Huber–Mises cylinder. The planes are defined by normals

$$\mathcal{N}_i = (\mathbf{n}^{(i)}_1 \otimes \mathbf{n}^{(i)}_2)_s, \quad i = 1, 2. \tag{5.20}$$

The concept of multiple potential surfaces forming a vertex on the smooth yield surface was studied earlier by MRÓZ [5] within the framework of non-associated flow laws.

According to (5.3) and (5.14) the unit normals

$$\mathbf{N}_i = \frac{\mathcal{N}_i}{\|\mathcal{N}_i\|} \tag{5.21}$$

can be expressed in the system of the unit vectors $(\mathbf{N}, \mathbf{T})$ attached at the loading point in the state of pure shear

$$\begin{aligned} \mathbf{N}_1 &= \cos 2\beta\mathbf{N} + \sin 2\beta\mathbf{T}, \\ \mathbf{N}_2 &= \cos 2\beta\mathbf{N} - \sin 2\beta\mathbf{T}. \end{aligned} \tag{5.22}$$

To obtain a geometrical visualization of the plastic potential functions, we can consider a three-dimensional space whose orthonormal base vectors $(\mathbf{i}_1, \mathbf{i}_2, \mathbf{i}_3)$ coincide with the principal directions of stress tensor. This is depicted in Fig. 2, where it is visible that the potential planes intersect along the generator of the Huber - Mises cylinder. The line of intersection corresponds to the locus of pure shear states in plane strain. The projection of the Huber–Mises cylinder and the potential planes onto the so-called π-plane (deviatoric plane) is displayed in Fig. 3. A two-dimensional coordinate system defined on the π-plane is used: the vertical axis with the unit vector $\mathbf{k}_2$ is taken to be the projection of the first principal stress axis on the π-plane τ_1' and the horizontal axis with the unit vector $\mathbf{k}_1$ is perpendicular to it. Then any stress tensor in that space can be expressed as

$$\boldsymbol{\tau} = \tau_1 \mathbf{i}_1 \otimes \mathbf{i}_1 + \tau_2 \mathbf{i}_2 \otimes \mathbf{i}_2 + \tau_3 \mathbf{i}_3 \otimes \mathbf{i}_3 \tag{5.23}$$

and its projection onto the π-plane as

$$\boldsymbol{\tau}' = \tau_x' \mathbf{k}_1 \otimes \mathbf{k}_1 + \tau_y' \mathbf{k}_2 \otimes \mathbf{k}_2, \tag{5.24}$$

where

$$\begin{aligned} \tau_x' &= -\frac{\tau_2}{\sqrt{2}} + \frac{\tau_3}{\sqrt{2}}, \\ \tau_y' &= \frac{2\tau_1}{\sqrt{6}} - \frac{\tau_2}{\sqrt{6}} - \frac{\tau_3}{\sqrt{6}}. \end{aligned} \tag{5.25}$$

Also the unit vectors $\mathbf{N}$, $\mathbf{T}$ and the normals $\mathbf{N}_i$, $i = 1, 2$ can be expressed as follows:

$$\begin{aligned} \mathbf{N} &= \frac{1}{2}\mathbf{k}_1 + \frac{1}{2}\sqrt{3}\mathbf{k}_2, \\ \mathbf{T} &= -\frac{1}{2}\sqrt{3}\mathbf{k}_1 + \frac{1}{2}\mathbf{k}_2, \end{aligned} \tag{5.26}$$

and

$$\begin{aligned} \mathbf{N}_1 &= \frac{1}{2}(\cos 2\beta - \sqrt{3}\sin 2\beta)\mathbf{k}_1 + \frac{1}{2}(\sqrt{3}\cos 2\beta + \sin 2\beta)\mathbf{k}_2, \\ \mathbf{N}_2 &= \frac{1}{2}(\cos 2\beta + \sqrt{3}\sin 2\beta)\mathbf{k}_1 + \frac{1}{2}(\sqrt{3}\cos 2\beta - \sin 2\beta)\mathbf{k}_2. \end{aligned} \tag{5.27}$$

Accordingly, the relations for the projections of the potential planes g_1 and g_2 onto the π-plane read

$$\begin{aligned} g_1: &\quad (\cos 2\beta - \sqrt{3}\sin 2\beta)\tau_x' + (\sqrt{3}\cos 2\beta + \sin 2\beta)\tau_y' - \sqrt{3}\kappa = 0, \\ g_2: &\quad (\cos 2\beta + \sqrt{3}\sin 2\beta)\tau_x' + (\sqrt{3}\cos 2\beta - \sin 2\beta)\tau_y' - \sqrt{3}\kappa = 0. \end{aligned} \tag{5.28}$$

If we take as an example a particular value of the misorientation angle $\beta = 15°$, what could be a good approximation, the relations (5.28) take the following simple form

$$\begin{aligned} g_1: &\quad 2\tau_y' - \sqrt{3}\kappa = 0, \\ g_2: &\quad \sqrt{3}\tau_x' + \tau_y' - \sqrt{3}\kappa = 0. \end{aligned} \tag{5.29}$$

The extensions of the planes of the potential functions g_1 and g_2 into the region outside the Huber–Mises yield locus delimit the *fully active range*. At the same time, the normals $\mathbf{N}_1$ and $\mathbf{N}_2$ to the potential planes g_1 and g_2 form a plastic wedge-shaped region that can be understood as an equivalent to the *eigencone* associated with the *extremal cone* discussed in [35].

The precise connection of the *fully active range* and *partially active range* with the geometric pattern of micro-shear bands makes possible to specify the relation for the rate of plastic deformations (5.19) for different loading paths. The normalization factor Λ can be expressed as

$$\Lambda = \|\mathring{\tau}' - (\mathring{\tau}' : \mathbf{N})\mathbf{N}\|^{-1}, \tag{5.30}$$

where

$$\|\mathring{\tau}' - (\mathring{\tau}' : \mathbf{N})\mathbf{N}\|^2 = \mathring{\tau}' : \mathring{\tau}' - (\mathring{\tau}' : \mathbf{N})^2. \tag{5.31}$$

Accounting for the angle α, which the loading direction (stress rate $\mathring{\tau}'$) forms with the normal $\mathbf{N}$

$$\mathring{\tau}' : \mathbf{N} = \|\mathring{\tau}'\| \cos\alpha, \tag{5.32}$$

and due to (5.31) and (5.32), the factor Λ reads

$$\Lambda = \frac{1}{\|\mathring{\tau}'\| \sin\alpha}. \tag{5.33}$$

Then in the *partially active range*, i.e. for $\alpha \in [\alpha_c, \frac{\pi}{2}]$, the equation for rate of plastic deformations (5.19) takes form

$$\mathbf{D}^p = \frac{(\mathring{\tau} : \mathbf{N})}{2h}\mathbf{N} + \frac{(\mathring{\tau} : \mathbf{N})}{2h}\frac{(f_{MS}^{(2)} - f_{MS}^{(1)})\tan 2\beta}{\|\mathring{\tau}'\| \sin\alpha}[\mathring{\tau}' - (\mathring{\tau} : \mathbf{N})\mathbf{N}]. \tag{5.34}$$

REMARK 4

It is interesting to observe that the derived relation (5.34) corresponds to a special case of the thoroughly nonlinear plastic flow laws studied earlier, within the framework of infinitesimal strains, by KLYUSHNIKOV [8], HILL [9], ILYUSHIN [10] and MRÓZ [11]. In our case the nonlinearity in the rate of stress is produced by the active micro-shear bands forming the definite spatial pattern.

The critical angle α_c, delimiting the *fully active range*, can be related with the geometry of micro-shear bands displayed in Fig. 1, $\alpha_c \leq 2\varphi = \frac{\pi}{2} - 2\beta$. In general, the interdependence of the active mechanisms of plastic deformation can be considered and in such a case the critical angle $\alpha_c < 2\varphi$. In the simplest case, however, if we assume that the active mechanisms of plastic flow are independent, the equality holds $\alpha_c = 2\varphi$. This results in

$$\Lambda = \frac{1}{\|\mathring{\tau}'\| \cos 2\beta}, \qquad \mathring{\tau} : \mathbf{N} = \|\mathring{\tau}'\| \sin 2\beta \tag{5.35}$$

and for continued plastic flow with the deviations from proportional loading that are contained within the *fully active range*, i.e. for $\alpha \in [0, 2\varphi]$, the relation for rate of plastic deformations (5.34) with an account of (5.35) transforms into the following one

$$\mathbf{D}^p = \frac{1}{2h}(\mathring{\tau} : \mathbf{N})\mathbf{N} + \frac{1}{2\mu}[\mathring{\tau}' - (\mathring{\tau} : \mathbf{N})\mathbf{N}], \tag{5.36}$$

where

$$\frac{1}{2\mu} = \frac{1}{2h}(f_{MS}^{(1)} - f_{MS}^{(2)})\tan^2 2\beta. \tag{5.37}$$

The second term in (5.34) and (5.36), denoted $\mathbf{D}_T$, is responsible for the non-coaxiality between the principal directions of stress and rate of plastic deformations. The term μ in (5.36) plays the role of the non-coaxiality modulus, that is formally similar to the Mandel–Spencer non-coaxiality modulus discussed by NEMAT-NASSER *et al.* [6], NEMAT-NASSER [7] and LORET [8] within the context of plastic behaviour of single crystals or geological materials.

If $\lambda \leq 0$, $\dot{\gamma}^* = 0$ and $\mathbf{D}^p = \mathbf{0}$. Observe that $\mathbf{D}_T = \mathbf{0}$ if $f^{(1)}_{MS} = f^{(2)}_{MS}$ or $\varphi = \pi/4$. The following special cases can be considered:

(i) for $\beta > 0$, and $f^{(1)}_{MS} \gtrless f^{(2)}_{MS}$ $\quad \mathbf{D}^p = \dfrac{1}{2h}(\overset{\circ}{\boldsymbol{\tau}} : \mathbf{N})\mathbf{N} \pm \mathbf{D}_T$;

(ii) for $\beta < 0$, and $f^{(1)}_{MS} \gtrless f^{(2)}_{MS}$ $\quad \mathbf{D}^p = \dfrac{1}{2h}(\overset{\circ}{\boldsymbol{\tau}} : \mathbf{N})\mathbf{N} \mp \mathbf{D}_T$.

To specify the relation for plastic spin the orientation tensor $(\mathbf{e}_1 \otimes \mathbf{e}_2)_a$ in (5.8) is eliminated and the following relation is derived with use of $(5.9)_1$

$$(\mathbf{e}^{(1)}_1 \otimes \mathbf{e}^{(1)}_2)_s \mathbf{D}^p - \mathbf{D}^p (\mathbf{e}^{(1)}_1 \otimes \mathbf{e}^{(1)}_2)_s = -\sin 2\beta (\dot{\gamma}^{(1)}_{MS} + \dot{\gamma}^{(2)}_{MS})(\mathbf{e}^{(1)}_1 \otimes \mathbf{e}^{(1)}_2)_a. \tag{5.38}$$

Hence, the equation for plastic spin reads

$$\mathbf{W}^p = \frac{1}{2\bar{\tau} \sin 2\beta}(\mathbf{D}^p \boldsymbol{\tau} - \boldsymbol{\tau} \mathbf{D}^p), \tag{5.39}$$

or with use of (5.34) and (5.36)

$$\mathbf{W}^p = \frac{f^{(2)}_{MS} - f^{(1)}_{MS}}{4\bar{\tau} h \cos 2\beta} \frac{(\overset{\circ}{\boldsymbol{\tau}} : \mathbf{N})}{\|\overset{\circ}{\boldsymbol{\tau}}'\| \sin 2\alpha}(\boldsymbol{\tau}\overset{\circ}{\boldsymbol{\tau}} - \overset{\circ}{\boldsymbol{\tau}}\boldsymbol{\tau}), \quad \text{for} \quad \alpha \in \left[\alpha_c, \frac{\pi}{2}\right], \tag{5.40}$$

and

$$\mathbf{W}^p = \frac{f^{(2)}_{MS} - f^{(1)}_{MS}}{4\bar{\tau} h \cos 2\beta} \tan 2\beta (\boldsymbol{\tau}\overset{\circ}{\boldsymbol{\tau}} - \overset{\circ}{\boldsymbol{\tau}}\boldsymbol{\tau}), \quad \text{for} \quad \alpha \in [0, \alpha_c]. \tag{5.41}$$

Observe that the effect of non-coaxiality and the related plastic spin appears only in the case when the discussed double-shearing system is non-symmetric with respect to the fractions $f^{(1)}_{MS}$, $f^{(2)}_{MS}$. Therefore, the model with the single shear system representing the nett fraction of the rate of plastic shearing $f = f^{(1)}_{MS} - f^{(2)}_{MS}$ can adequately describe plastic flow accounting for micro-shear bands. The pertinent equations for the rate of plastic deformations can be obtained by replacing in (5.34) and (5.36) as well as in (5.40) and (5.41) the term $f^{(1)}_{MS} - f^{(2)}_{MS}$ with f.

6. Discussion and concluding remarks

The fractions $f^{(1)}_{MS}$, $f^{(2)}_{MS}$ and in particular the nett fraction f can be considered as internal variables displaying the stochastic character of the active shear bands formations during the deformation process. Proper description of their evolution remains an open and challenging problem worth further studies. In particular, the experimental observations of possible fractal character of the organization of the active micro-shear bands in time and space are required (the importance of this problem was stressed in [24] and some preliminary results are mentioned in [14]). Certain microscopic models lead to the

conjecture that shear banding can contribute to the rate of plastic deformations as a sequence of generations of active micro-shear bands governed by logistic equation (Verhults equation), taken from the population dynamics, (cf. [2]).

The assessment of the possible incorporation of the rate of plastic deformation given by (5.34) or (5.36) into an elastic-plastic material model can be made basing on the discussion of the significance of the rigid-plastic theory for plane strain in relation to a compressible elastic-plastic solid provided in [39], p. 129 and in CHAKRABATRY [49], p.409. For plane strain within an elastic region, component normal to the plane of deformation reads

$$\tau_z = \nu(\tau_1 + \tau_2). \tag{6.1}$$

Due to (5.1) and (5.2), the discontinuities of the stress components at the elastic-plastic boundary for the values of the Poisson's ratio that are different from $\nu = 0.5$ can be expected. The elasto-plastic model based on the derived rate of plastic deformations is rigorously true for the case of elastic incompressibility, i.e. for $\nu = 0.5$. However, τ_z approaches the value given in (5.1) as the magnitude of the in-plane principal plastic strains progressively increases. Therefore, the discussed elasto-plastic model can be considered as an approximation that holds increasingly well within the plastic zone, but may be appreciably in error over a region bordering the elasto-plastic interface or in the case when significant change in strain path occurs (cf. [39], p. 79 for the pertinent discussion of the example of compression under condition of plane strain).

The new relations for plastic flow laws accounting for micro-shear banding can be applicable in modelling of large plastic deformations under highly constrained conditions, which appear in technological shaping processes or in the case of postcritical behaviour and ductile failure, while coalescence of voids occurs. In the latter case, the implementation of the presented equations into the known theories of materials with internal imperfections, PERZYNA [60], or models describing the porous material failure by void growth to coalescence, TVERGAARD [61], to describe the matrix material can lead to more accurate predictions of damage processes.

The derived constitutive equations make a basis for the formulation of a more general three-dimensional model. The question arises then how varying loading paths affect the spatial pattern, and in particular the misorientation angle β, of the active micro-shear bands? Further experimental and theoretical studies are necessary to shed more light on this important problem.

Acknowledgement

The first stage of this work was performed while the author was visiting at, and supported by the Department of Solid Mechanics of the Technical University of Denmark; and the later stages were completed with the support of the Committee for Research (KBN) Poland, under the project No. 3 1112 91 01. Fruitful discussions with Prof. Viggo TVERGAARD and his critical comments are greatly appreciated.

References

1. H.E. DÈVE and R.J. ASARO, *The development of plastic failure modes in crystalline materials: shear bands in fcc polycrystals*, Metall. Trans., **20A**, 5, 59–593, 1989.
2. R.B. PĘCHERSKI, *A model of plastic flow with an account of micro-shear banding*, ZAMM, **72**, T250–T254, 1992.

3. R.B. PĘCHERSKI, *Physical and theoretical aspects of large plastic deformations involving shear banding*, 167–178, [in:] Proc. IUTAM — Symposium on Finite Inelastic Deformations. Theory and Applications, D. BESDO and E. STEIN [Eds.], Springer Verlag, 1992.
4. R.B. PĘCHERSKI, *A model of plastic flow accounting for micro-shear bands idealized by means of double-shearing system*, ZAMM, T339–T343, 1993.
5. Z. MRÓZ, *Non-associated flow laws in plasticity*, J. de Mécanique, **2**, 21–42, 1963.
6. S. NEMAT-NASSER, M.M. MEHRABADI and T. IWAKUMA, *On certain macroscopic and microscopic aspects of plastic flow of ductile materials*, 157–172, [in]: Three-Dimensional Constitutive Relations And Ductile Fracture, S. NEMAT-NASSER [Ed.], North-Holland, 1981.
7. S. NEMAT-NASSER, *Generalization of the Mandel-Spencer double-slip model*, 269–282, [in]: Large Deformations of Solids: Physical basis and Mathematical Modelling, J. GITTUS, J. ZARKA and S. NEMAT-NASSER [Eds.], Elsevier, London, New-York, 1986.
8. B. LORET, *Some macroscopic consequences of the granular structure of sand*, 477–496, ibid.
9. V.D. KLYUSHNIKOV, *On the possible way of formulating physical relations in plasticity* [in Russian], Prikl. Math. Mech., **23**, 282–291, 1959.
10. R. HILL, *Some basic principles in the mechanics of solid without a natural time*, J. Mech. Phys. Sol., **7**, 209–225, 1959.
11. A.A. ILYUSHIN, *Plasticity* [in Russian], Moscow 1964.
12. Z. MRÓZ, *On non-linear flow laws in the theory of plasticity*, Bull. Acad. Polon. Sci., **12**, 531–539, 1964.
13. H. NEUHÄUSER, *Slip-line formation and collective dislocation motion*, [in]: Dislocations in Solids, 319–440, vol. 6, F.R.N. NABARRO, [Ed.] North-Holland, Amsterdam 1983.
14. H. NEUHÄUSER, *The dynamics of slip band formation in single crystals*, Res. Mechanica, **23**, 113–135, 1988.
15. J. GIL SEVILLANO, P. VAN HOUTTE and E. AERNOUDT, *Large strain work hardening and textures*, Progress in Materials Science, **25**, 69–412, Pergamon Press, 1981.
16. J.D. EMBURY, A. KORBEL, V.S. RAGHUNATHAN and J. RYS, *Shear band formation in cold rolled* Cu-6% *Al single crystals*, Acta Metall., **32**, 1883–1894, 1984.
17. M. HATHERLY and A.S. MALIN, *Shear bands in deformed metals*, Scripta Metall., **18**, 449–454, 1984.
18. A. KORBEL, J.D. EMBURY, M. HATHERLY, P.L. MARTIN and H.W. ERBSLOH, *Microstructural aspects of strain localization in* Al-Mg *alloys*, Acta Metall., **34**, 1999–2009, 1986.
19. S.V. HARREN, H.E. DÈVE and R.J. ASARO, *Shear band formation in plane strain compression*, Acta Metall., **36**, 2435–2480, 1988.
20. A. KORBEL, P.L. MARTIN, *Microstructular events of macroscopic strain localization in prestrained tensile specimens*, Acta. Metall., **36**, 2575, 1988.
21. A. KORBEL, *The real nature of shear bands — plastons?*, [in:] Plastic Instability, Proc. Int. Symp. on Plastic Instability. Considère Memorial (1841–1914), Presses de l'Ecole Nationale des Ponts et Chaussées, Paris, 325–335, 1985.
22. M. SZCZERBA and A. KORBEL, *Strain softening and instability of plastic flow in* Cu-Al *single crystals*, Acta Metall., **35**, 1129–1135, 1987.
23. W.BOCHNIAK, *The microstructure of Lüders band in* Cu-Sn2 *alloy*, Scripta Metall., **23**, 519–522, 1989.
24. A. PAWEŁEK and A. KORBEL, *Soliton-like behaviour of a moving dislocation group*, Phil. Mag., **61B**, 829–842, 1990.
25. B.J. DUGGAN, M. HATHERLY, W.B. HUTCHINSON and P.T. WAKEFIELD, *Deformation structures and textures in cold-rolled* 70:30 *brass*, Metal Sci., **12**, 343–351, 1978.
26. P. DUBOIS, *Etude cristallographique de l'initiation et de la propagation de bandes de cisaillement dans les metaux purs*, These présenté a l'Université Paris-Nord pour obtenir le grade de Docteur, Juin 1988.
27. P. DUBOIS, M GASPERINI, C. REY and A. ZAOUI, *Crystallographic analysis of shear bands initiation and propagation in pure metals. Part II. Initiation and propagation of shear bands in pure ductile rolled polycrystals*, Arch. Mech., **40**, 35–40, 1988.
28. S. YANG, *Etude experimentale et theoretique de línitiation de de deformation plastique en bande de cisaillement dans les materiaux metalliques*, These présenté a l'Université Paris-Nord pour obtenir le grade de Docteur, November 1990.
29. C. REY, private communication.
30. W. Y. YEUNG and B.J. DUGGAN, *On the plastic strain carried by shear bands in cold-rolled* α*-brass*, Scripta Metall., **21**, 485–490, 1987.
31. L. ANAND and W.A. SPITZIG, *Initiation of localized shear bands in plane strain*, J. Mech. Phys. Solids, **28**, 113–128, 1980.

32. R. HILL, *The mechanics of quasi-static plastic deformation in metals*, [in]: Surveys in Mechanics, 7–31, G.K. BATCHELOR, R.M. DAVIES [Eds.], Cambridge, 1956.
33. K. HAVNER, *On the mechanics of crystalline solids*, J. Mech. Phys. Solids, **21**, 383–394, 1973.
34. K. HAVNER, *Aspects of theoretical plasticity at finite deformation and large pressure*, ZAMP, **25**, 765–781, 1974.
35. R. HILL, *The essential structure of constitutive laws for metal composites and polycrystals*, J. Mech. Phys. Solids, **15**, 779–95, 1967.
36. R. HILL, *On constitutive macro-variables for heterogeneous solids at finite strain*, Proc. R. Soc. Lond., **A 326**, 131–147, 1972.
37. J. MANDEL, *Plasticité classique et viscoplasticité*, C.I.S.M., Udine, Springer-Verlag, 1972.
38. R. HILL and J.R. RICE, *Constitutive analysis of elastic-plastic crystals at arbitrary strain*, J. Mech. Phys. Solids, **20**, 401–413, 1972.
39. H. PETRYK, *On constitutive inequalities and bifurcation in elastic-plastic solids with a yield-surface vertex*, J. Mech. Phys. Solids, **37**, 265–291, 1989.
40. C. STOLZ, *On relationship between micro and macro scales for particular cases of nonlinear behaviour of heterogeneous media*, 617–628, [in:] Proc. of IUTAM/ICM Symposium on Yielding, Damage and Failure of Anisotropic Solids, J.-P. BOEHLER [Ed.], Mechanical Engineering Publications, London 1990.
41. C. TEODOSIU, *A dynamic theory of dislocations and its applications to the theory of the elastic-plastic continuum*, [in]: Fundamental Aspects of Dislocation Theory, A. SIMMONS *et. al.* [Eds.], Nat. Bur. Stand. Spec. Publ. 317, II, 837–875, 1970.
42. J. KRATOCHVIL, *Finite-strain theory of crystalline elastic-inelastic materials*, J. Appl. Phys., **42**, 1104–1108, 1971.
43. M. KLEIBER and B. RANIECKI, *Elastic-plastic materials at finite strains*, [in]: Plasticity Today, Modelling, Methods and Applications, A. SAWCZUK and G. BIANCHI [Eds.], Proc. Int. Symp. on Current Trends and Results in Plasticity, CISM, Unide, Italy, June 1983, Elsevier, London–N. York, 3–46, 1985.
44. B. RANIECKI and S.K. SAMANTA, *The thermodynamic model of rigid-plastic solid with kinematic hardening, plastic spin and orientation variables*, Arch. Mech., **41**, 747–758, 1989.
45. B. RANIECKI, Z. MRÓZ, *On the strain-incluced anisotropy and texture finite strain of rigid-plastic solids*, **13**–32, [in]: Inelastic Solids and Structures, A. Sawczuk Memorial Volume, M. KLEIBER and A. KÓNIG [Eds.], Pineridge Press, Swansea 1990.
46. S. CLEJA-TIGOIU and E. SOÓS, *Elastoviscoplastic models with relaxed configurations and internal state variables*, Appl. Mech. Rev., **43**, 131–151, 1990.
47. B. RANIECKI and H.V. NGUYEN, *Isotropic elastic-plastic solids at finite strain and arbitrary pressure*, Arch. Mech., **36**, 687–704, 1984.
48. R.B. PĘCHERSKI, *The plastic spin concept and the theory of finite plastic deformations with induced anisotropy*, Arch. Mech., **40**, 807–818, 1988.
49. R. LAMMERING, E. STEIN and R.B. PĘCHERSKI, *Theoretical and computational aspects of large plastic deformations involving strain-induced anisotropy and developing voids*, Arch. Mech., **42**, 347–375, 1990.
50. R. HILL, *Theoretical plasticity of textured aggregates*, Math.Proc. Camb. Phil. Soc., **85**, 179–191, 1979.
51. S.S. HECKER, *Experimental studies of yield phenomena in biaxially loaded metals*, [in]: Constitutive Equations in Viscoplasticity: Computational and Engineering Aspects, J.A. STRICKLIN, K. J. SACZALSKI [Eds.], ASME, AMD, **20**, 1–33, 1976.
52. K. IKEGAMI, *Experimental plasticity on the anisotropy of metals*, [in] Mechanical Behaviour of Anisotropic Solids, Proc. of the Euromech Colloquium 115, Villard-de-Lans, June 19–22, 1979, J.P. BOEHLER [Ed.], Martinus Nijhoff, 201–242, 1982.
53. R. HILL, *Eigenmodal deformations in elastic-plastic continua*, J. Mech. Phys. Solids, **15**, 371–386, 1967.
54. Z. MRÓZ and A. NIEMUNIS, *On the description of deformation anisotropy of materials*, [in:] Yielding, Damage, and Failure of Anisotropic Solids, Proc. of the IUTAM/ICM Symposium Antoni Sawczuk in Memoriam, Villard-de-Lans, 24-28 August 1987, J.P. BOEHLER [Ed.], Mechanical Engineering Publications Ltd., London, 171–186, 1990.
55. R. HILL, *The mathematical theory of plasticity*, Clarendon Press, Oxford 1956.
56. J. CHRISTOFFERSEN, J.W. HUTCHINSON, *A class of phenomenological corner theories of plasticity*, J. Mech. Phys. Solids, **27**, 465–487, 1979.
57. B. DODD and Y. BAI, *Ductile fracture and ductility with applications to metalworking*, Academic Press, London 1987.

58. H.M. ZBIB, *On the mechanics of large inelastic deformations: noncoaxiality, axial effects in torsion and localization*, Acta Mech., **87**, 179–196, 1991.
59. J. CHAKRABARTY, *Theory of plasticity*, McGraw-Hill, Singapore 1987.
60. P. PERZYNA, *Constitutive modelling of dissipative solids for postcritical behavior and fracture*, J. Engng. Materials and Technology, **106**, 410–419, 1984.
61. V. TVERGAARD, *Material failure by void growth to coalescence*, [in:] Advances in Applied Mechanics, J.W. HUTCHINSON and T.Y. WU [Eds.], Academic Press, New York, 83–151, 1990.

POLISH ACADEMY OF SCIENCES
INSTITUTE OF FUNDAMENTAL TECHNOLOGICAL RESEARCH.

Received July 31, 1992.